arXiv:1304.1615v1 [cond-mat.mtrl-sci] 5 Apr 2013

# Redistribution of Fermi level density of states in nickelate superlattices without charge transfer

Myung Joon Han[1, 2, 3, *] and Michel van Veenendaal[2, 3]

[1]*Department of Physics, Korea Advanced Institute of Science and Technology, Daejeon 305-701, Korea*
[2] *Department of Physics, Northern Illinois University, De Kalb, Illinois 60115, USA*
[3]*Advanced Photon Source, Argonne National Laboratory, Argonne, Illinois 60439, USA*

(Dated: April 8, 2013)

In the layer-by-layer controlled artificial structure of transition-metal oxides, it is known that the transition metal $d$ charge valence, orbital occupation, and other degrees of freedom are often reconstructed, which can lead to unexpected material properties such as a highly metallic interface, magnetism, and superconductivity. In this study, by using first-principles density functional theory calculations for $(\mathrm{LaNiO_3})_m/(\mathrm{SrTiO_3})_n$ superlattices, we report a different type of reconstruction caused by the heterostructuring, that is, redistribution. The Fermi level density of states of metallic nickelate layers is significantly reduced without charge transfer in the vicinity of interface to the insulating $\mathrm{SrTiO_3}$. Further analysis indicates that this systematic way of electron response can be a general feature particularly in the nickelate systems. Our result sheds new light towards understanding the nickelates and other transition-metal oxide heterostructures.

## I. INTRODUCTION

Recent advances in the layer-by-layer growth technique of transition-metal oxide (TMO) heterostructures have created considerable research interest [1]. In these artificially structured interfaces, many exotic material characteristics have been reported that are strikingly different from the bulk properties and from the characteristics of a typical semiconducting interface (non-TMO interface) [2]. For example, early studies of Ti-based superlattices such as $\mathrm{LaTiO_3/SrTiO_3}$ (LTO/STO) and $\mathrm{SrTiO_3/LaAlO_3}$ (STO/LAO) have revealed that heterostructuring induces unique electronic processes in TMOs that can dramatically change the macroscopic material properties [3–6]. In these cases, it is widely believed that the valence charge reconstruction and the polar discontinuity can drive the interfaces to be metallic even if the two mother materials are good insulators. The orbital degrees of freedom are also found to be reconstructed at the interface between manganite and cuprate [7]. Other examples of emergent material properties caused by the heterostructure geometry include superconductivity [8] and magnetism [9, 10]. These new findings raise the important question how the heterostructuring of TMO materials affects the density of states (DOS) close to the Fermi level and the related low-energy properties.

In this study, we report a new type of interface phenomenon: Fermi level DOS modulation caused by the state redistributions without valence change. Although this phenomenon exhibits similarities to the charge reconstruction and orbital reconstruction, it displays distinctive characteristics. We found that the Fermi level DOS strongly modulates as a function of the location of nickel atoms relative to the interface. Our first-principles calculations of $\mathrm{LaNiO_3}$ (LNO)/STO clearly demonstrate that this novel electronic modulation around the Fermi level is intrinsic to the structure itself, *i.e.,* the heterostructuring of nickelates, and not originating due to the other effects such as the charge transfer, oxidation of Ni and valence change. Further analysis strongly indicates that this kind of behavior can be a universal feature in nickelate superlattices sandwiched by *any* wide-gap material. Our result sheds new light on the understanding of TMO interface phenomena.

It should be emphasized that our system $(\mathrm{LNO})_m/(\mathrm{STO})_n$ is distinctive from a widely-studied system, LNO/LAO, due to the possibility that Ti can have active $d$ electrons around the Fermi level. The charge transfer can in principle take place between Ti and Ni. As an example, it would be instructive to compare LNO/STO to LNO/LTO superlattice in which the Ti can clearly have an electron in its $d$ orbitals, and there may be the electron transfer from Ti to Ni, leading to the configuration of Ti as $d^{0+\delta}$ (or $d^{1-\delta}$ depending on the amount of charge transfer) and Ni as $d^{8-\delta}$ (or $d^{7+\delta}$). This kind of charge transfer is basically the mechanism that drives the exchange bias effect in the LNO/$\mathrm{LaMnO_3}$ (LMO) [11]. However, in our case LNO/STO, it is not at all clear if such an electron transfer would take place especially for the case of $m$=$n$=1. Note that $(\mathrm{LNO})_1/(\mathrm{STO})_1$ can also be identified as $(\mathrm{SrNiO_3})_1/(\mathrm{LTO})_1$, and this alternative specification of the system implies that Ti has $d^1$ (LTO-like) configuration instead of $d^0$ (STO-like). As we will show in the below, this possibility is not realized and Ti remains as $d^0$ even in the $m$=$n$=1 case, and Ni as $d^7$ (we drop off the indication of ligand hole for simplicity). From this interesting new finding, important questions arise: If there is no charge transfer between the transition metal (TM) ions, what happens at the interface? In other words, under the condition that no charge transfer is allowed, what kind of response can

---

*Electronic address: mj.han@kaist.ac.kr

be made by the metallic material, LNO, in the vicinity of interface to the insulating STO? The interface Ni would exhibit the same characteristics with the inner layer Ni? If not, what kind of possibility does Ni have in this superlattice geometry? This is a well defined open question that has never been addressed before.

Our calculations show that the Ni-$d$ electrons are actually adjusted at the interface in a systematic way that its DOS is redistributed while keeping the same total number of electrons. That is, the interface Ni, closer to the insulating STO, becomes more insulator-like in the sense that its Fermi level DOS gets reduced while the inner layer Ni more metal-like in the sense that the more DOS at the Fermi energy. And, we suggests, this DOS redistribution process can be understood from a simple picture based on the interactions between the heterostructuring-induced molecule-like states.

## Result

### Classification of Ni types and modulation of Fermi level DOS

Let us start with a classification of nickel sites in LNO/STO considering their local environments; nickel can be located either in between two $La^{3+}O^{2-}$ layers or in between the $La^{3+}O^{2-}$ and $Sr^{4+}O^{2-}$ layers. Further, its neighboring TM can be either titanium or nickel (see the inset of Fig. 1). If a nickel ion is located in between two $La^{3+}O^{2-}$ layers and its two neighboring TM sites are both Ni, it is bulk-like. However, at the interface, there are three different local structures. Let us denote these three interfacial types as I1, I2, and I3 (see the inset of Fig. 1). As the electronic structure of Ni can be affected by both these two factors (the neighboring TM ions and the ionic potentials caused by $A$-site cations), it is important to understand these effects on the Ni electronic structures. We will discuss this point below in further detail.

Recent depth-resolved standing-wave x-ray photoemission spectroscopy (SWXPS) studies [12] show that the near-Fermi-level nickel states in $(LNO)_4/(STO)_3$ are significantly suppressed at the interface. A detailed analysis of the angular behavior of the SWXPS spectra indicates that the electronic states are suppressed at the two outer LNO layers adjacent to the STO layers (type I2 and I3 nickel in our definition), but not in the inner layers (bulk-like nickel). It was speculated in Ref. 12 that the variation in Fermi level DOS could be due to the different oxidation of Ni ions; however, no further experimental evidence or explanation was provided.

### DOS redistribution without charge transfer

We note that a clear understanding of this DOS modulation is of significant importance. If there is a charge transfer between TM ions, it is quite natural to expect that the amount of DOS changes at the Fermi level. Interestingly, however, our calculation shows that such a charge transfer and oxidation process are not responsible for this DOS modulation. We performed extensive calculations for $(LNO)_m/(STO)_n$ with $(m, n) = (1, 1), (2, 2), (3, 3), (4, 1), (4, 3)$, and $(5, 2)$, and found that the number of $e_g$ electrons is 2.36–2.39 regardless of the type of nickel. From the point of view that all the nickels remain in the same charge status, the observed DOS modulation is quite unexpected and hard to be explained by any of the ‘reconstruction’ processes that were suggested before.

The fact that there is no valence change or further oxidation of Ni is most dramatically seen in $m$=$n$=1 case for which the alternative characterization of the superlattice as $(SNO)_1/(LTO)_1$ is also possible if the charge transfer might really happen. Since Ti has $d^1$ configuration in LTO while $d^0$ in STO, the result can be most clearly seen in the Ti states. The calculated Ti-$d$ DOS in Fig. 2(b) shows that all the Ti-$d$ states are empty. Therefore one can safely identify the system as $(LNO)_1/(STO)_1$, and there is no charge transfer between Ni and Ti even in the $m$=$n$=1 case.

The same point is also confirmed by that the effect of $A$-site cation potential asymmetry (*i.e.,* $Sr^{4+}$ versus $La^{3+}$) does not cause any significant change in the electronic structure. This effect can be studied by examining the (3,3) heterostructure, for example, that contains both type I2 and I3 nickel ions (compare the dotted-blue with dashed-green line in Fig. 3(b)). Since the two nickel ions only differ due to the $A$-site cations, the different electronic structure reflects the effect due to the $A$-site asymmetry. Figure 3(b) shows that the DOS change is very small. Therefore, the valence reconstruction is not relevant to this nickelate system presumably due to the strong covalency. In addition, for other ($m$,$n$) structures, the projected DOS for type I2 and I3 nickel is always similar (seen in Fig. 4(b) for the case of (5,2) or upon comparison of Fermi level DOS value at $z = 0$ and $z = 1$ in Fig. 1).

Now, considering that the nickel valence states are all same regardless of its position and the cation potential effect, it is quite surprising that the Fermi level DOS significantly varies. The calculated value of this quantity is summarized in Fig. 1 where the DOS values at the Fermi level (projected onto the different nickel sites) are plotted. It is clear that the interfacial nickel ions (see Fig. 1 where the $z$-position is normalized so that types I1, I2, and I3 located either at $z = 0$ or at $z = 1$) always have notably smaller Fermi level DOS than the bulk-like nickel sites ($0 < z < 1$ in Fig. 1). The Fermi level DOS is significantly enhanced for the bulk-like nickel ions. The difference becomes even more pronounced as the number of Ni layers increases from $m = 3$ to $m = 5$. For $m = 5$, the Fermi level DOS for the inner most layer Ni ions is larger by a factor $\sim$2 when compared with that of the interfacial one. Since there is no charge transfer and no valence change, but a strong DOS modulation at the Fermi level, DOS should be redistributed in such a way that the total number of electrons is kept same. The further analysis shows that DOS is actually redistributed in a systematic way so that the Fermi level DOS gradually decreases as the nickelate layer gets closer to the interface. In order to make the charge valence unchanged, this weight is transferred to the lower energy part as schematically shown in Fig. 4(a). It is interesting to note that the metallic LNO layers become more insulator-like when they come closer to the insulating STO, while keeping the same valence charge; *i.e.*, they try to have smaller number of states at the Fermi level. On the other hand, the inner LNO layers, far away from STO, become more metallic in the sense that they have more DOS at the Fermi level.

This process is schematically illustrated in Fig. 4(a), and Fig. 4(b) shows that the reduction of DOS is quite significant. As seen in Fig. 4(b), the $d_{3z^2-r^2}$ states of the inner most (B; bulk-like) nickel is much larger than the two interface nickels (I2 and I3). The arrow indicates the DOS reduction at the Fermi level. It is found that the reduced states are transfered to the lower energy parts in case of interface nickel sites (for the wider range plot and the integrated DOS are given in Supplementary Material).

### Mechanism of redistribution

It now became clear that the Fermi level DOS behaves in a systematic way of state redistributions while keeping the same total number of charge. The remaining question is how to understand (at least qualitatively) the mechanism behind the DOS modulation or redistribution process. We suggest a relatively simple picture can explain this novel interface phenomenon based on the interactions between the molecule-like quantum states formed by the heterostructure geometry. Let us go back to the $m$=$n$=1 case which serves as a starting point of our argument. The Ni-$e_g$ DOS for $m = n = 1$ superlattice is presented in Fig. 2(a). The important point here is that the bandwidth of $d_{3z^2-r^2}$ state is markedly narrower than that of the $d_{x^2-y^2}$ state. The smaller dispersion of $d_{3z^2-r^2}$ is due to the limited hybridization along the $z$ direction by the presence of STO layers. From this characteristics of $d_{3z^2-r^2}$ state, we can consider this state as remnants of the molecular orbital character arising from a chain of $m$ $d_{3z^2-r^2}$ orbitals along the $z$ direction. These molecular-orbital-like features are further confirmed by the DOS shape of the (3,3) case; Figure 3(b) clearly shows the features related to the bonding, antibonding, and nonbonding states of the $m = 3$ chain. It is noted that the DOS of the bulk-type nickel (solid-red line) is strongest in the bonding and antibonding features at ∼0 and ∼2.2 eV.

This point is further supported by our tight-binding analysis, which captures the essence of the features found in the first-principles results. Assuming that the system can approximately be treated as a linear chain of $m$-molecular orbitals, we constructed a tight-binding model Hamiltonian corresponding to $N$ atoms, $H = \sum_{i=1}^{N} t c_i^\dagger c_j$, where $c_i^\dagger$ creates an electron at the $i$th site in the $z$ direction. The weight of the central (bulk-like) atom $|\langle i_c|E\rangle|^2$ is plotted in Fig. 3(a) as a function of energy $E$ (in the unit of $t$). As the chain length, $m$, increases from $m = 1$ to 3 and 5, the states interact with each other and spread out over a wide energy range. For $m = 3$, the two-peak feature of bonding and anti-bonding is most clearly seen, which is consistent with the results of our first-principles calculation in Fig. 3(b) (for the results of other $m$ values, see Supplementary Materials). Another important point in this analysis is that the bonding-peak position gradually shifts toward the lower energy region as $m$ increases, as marked by the asterisks in Fig. 3(a). Figure 3(c) clearly shows that this characteristic behavior of the lower energy part of the $d_{3z^2-r^2}$ states is also found in the first-principles calculations. As the number of layers increases, the peak position (marked by asterisks in Fig. 3(c)) shifts towards the lower energy region. It is the electronic origin that leads to a strong modulation in the number of states at the chemical potential shown in Fig. 1. Therefore, we can conclude that the characteristic modulation of Fermi level DOS is attributed to the formation of molecule-like quantum states induced by the blocking of hybridization along $z$ direction, and to the redistribution of DOS around the Fermi level caused by the interactions between these states.

### Discussion

There are crucial differences between the DOS modulation and the previously reported interface phenomena. In general, electronic [4] and orbital [7] reconstructions depend on the relative on-site energies of interfacial ions leading to a redistribution of charge between different sites and orbitals. In contrast, Fermi-level DOS modulations involve a strong redistribution of states within the same sites and the same orbitals due to the presence of the interface. The redistribution leads to a strong change in the contribution to the Fermi level DOS as a function of the position of the TM relative to the interface. Since the low-energy properties are mainly determined by the states close to the chemical potential, strong position-dependent electronic properties can be expected and macroscopic properties (*e.g.,* resistivity) should be sensitive to these strong modulations. The direct observation of this kind of electronic response is difficult as the charge valence of the interface remains unchanged, and only the near-Fermi-level DOS should be measured. However, we note that SWXPS measurements can be used for the verification of our results. Therefore, it is important to note that the results of a recent experiment by Kaiser and co-workers for ($m$=4, $n$=3) compares well with our conclusions [12].

Our analysis can be applied to other superlattice structures with LNO sandwiched by *any* wide-gap insulator in which the hybridization is also strongly blocked only along the $z$ direction. Therefore, the same type of DOS modulation should be found in the related heterostructures. To verify this point, we calculated the Fermi level DOS for $(\mathrm{LNO})_m/(\mathrm{LAO})_n$ with $(m, n) = (3, 3), (4, 1), (5, 2)$, and we found that the same modulations also occur in this different type of nickelate systems (for the plot comparable with Fig. 1, see Supplementary Material). These observations further confirm our analysis and conclusion. It is noteworthy that our tight-binding analysis based on the molecular-orbital chain model is better applied to the case of LNO/LAO. We can conclude that the DOS modulation can be a universal feature in nickelate superlattices and possibly also in other interfaces in between metals and insulators.

In addition, our results concerning the Fermi level DOS reduction at the interfaces can provide an interesting new picture of nickelate superlattices. It is noteworthy that the DOS reduction at the interface is observed for all the compositions of ($m \geq$3, $n$), while for $m \leq 2$, only the interface nickel ions exist and there is no bulk-like one. Interestingly, several experiments on the nickelate superlattice independently reports that the MIT occur at $m \approx 3$. The same critical thickness was commonly observed in the nickelate systems; LNO/STO [13], LNO/LAO [14], LNO/SrMnO$_3$ [15], and LNO/LMO [16]. It is therefore temping to relate the metallic and insulating phase to the bulk-like (B) and interface-like (I1, I2, I3) nickel layers in our classification, respectively, as the bulk-like nickel has more states at the Fermi energy and it start to appear at $m = 3$. Further, a recent experiment by Boris and co-workers reported that this MIT is accompanied with the paramagnetic to magnetic transition [14]. We note that, in the Kondo-type screening, the screening strength is governed by the Fermi level DOS as is clear from the Kondo temperature scale, $T_K \sim e^{-1/\rho_0 J_K}$, where $\rho_0$ refers to the Fermi level DOS. Therefore, it may be interesting to regard the nickelate superlattices based on our result as a kind of 'Kondo lattice' system where the enhanced Fermi level DOS is responsible for the metallic conduction and simultaneously for the screening of local magnetic moments (schematic illustration of this point can be found in Supplementary Material).

To summarize, we report a new type of interface phenomenon: Fermi level DOS modulation across the LNO layers in LNO/STO superlattice systems. We show that this modulation is an intrinsic effect caused by the heterostructuring itself without valence change or oxidation. It is related to but clearly distinctive from other intriguing interface phenomena such as orbital and charge reconstruction. Our analysis demonstrates that this novel electronic response to the hetero-interface structure originates from the novel process of quantum state formation and interactions between them. It can be responsible for MIT in the related systems, providing a new theoretical aspect to the complex-TMO research.

## Methods

For band structure calculations, we employed the norm-conserving pseudopotential with a partial core correction, and a linear combination of localized pseudo-atomic orbitals (LCPAO) as a basis set. We adopted the local density approximation (LDA) for the exchange-correlation energy functional as parametrized by Perdew and Zunger [17], and we used an energy cutoff of 400 Ry and k-grid of 12 × 12 × 6 per unit volume. It is noted that bulk LNO is a paramagnetic metal down to low temperatures and no studies yet have reported on the magnetic order in LNO/STO. Therefore, a conventional LDA calculation is appropriate for the LNO/STO system since a LDA+U type of calculation, for example, has to assume a long-range ordered magnetic phase. We used the Mulliken method for the charge analysis where the Kohn-Sham states are projected onto our LCPAO basis orbitals. It is noted that the number of Ni-$e_g$ electrons obtained in this study is in the range comparable to the case of LNO/LXO (X: B, Al, Ga, In) superlattice systems as reported in Ref. 18 [18]. The geometry relaxation has been performed with the force criterion of $10^{-3}$ Hartree/Bohr. During the relaxation process, we assume that the in-plane lattice constant does not change due to its pinning with the substrate (we assumed the STO lattice parameter for the substrate) [19].

## Acknowledgments

This work was supported by the U.S. Department of Energy (DOE), DE-FG02-03ER46097, and NIU's Institute for Nanoscience, Engineering, and Technology. The work at the Argonne National Laboratory was supported by the U.S. DOE, Office of Science, Office of Basic Energy Sciences under Contract No. DE-AC02-06CH11357.

## Supplementary Information

The details of the calculation techniques and further discussion of the electronic structure are linked to the online version of the paper.

## Author Contributions

M. J. Han performed the density functional theory calculations and M. van Veenedaal the tight binding calculations. All authors contributed in analyzing the results and writing the paper.

## Competing Interests

The authors declare that they have no competing financial interests.

---

[1] Mannhart, J., Blank, D. H. A., Hwang, H. Y., Millis, A. J. and Triscone, J. M. Two-Dimensional Electron Gases at Oxide Interfaces *Bulletin of the Materials Research Society* **33**, 1027 (2008).

[2] Hwang H. Y., Iwasa, Y., Kawasaki, M., Keimer, B., Nagaosa N. and Tokura Y. Emergent phenomena at oxide interfaces *Nature Mater.* **11**, 103 (2012).

[3] Ohtomo, A., Muller, D. A., Grazul, J. L. and Hwang, H. Y. Artificial charge-modulationin atomic-scale perovskite titanate superlattices *Nature* **419**, 378 (2002).

[4] Okamoto S. and Millis, A. J. Electronic reconstruction at an interface between a Mott insulator and a band insulator *Nature* **428**, 630 (2004).

[5] Ohtomo A. and Hwang, H. Y. A high-mobility electron gas at the LaAlO3/SrTiO3 heterointerface *Nature* **427**, 423 (2004).

[6] Nakagawa, N., Hwang, H. Y. and Muller, D. A. *Nature Materials* Why some interfaces cannot be sharp **5**, 204 (2006).

[7] Chakhalian, J., Freeland, J. W., Habermeier, H.-U., Cristiani, G., Khaliullin, G., van Veenendaal, M. and Keimer, B. Orbital Reconstruction and Covalent Bonding at an Oxide Interface *Science* **318**, 1114 (2007).

[8] Reyren, N., Thiel, S., Caviglia, A. D., Kourkoutis, L. F., Hammerl, G., Richter, C., Schneider, C. W., Kopp, T., Rüetschi, A.-S., Jaccard, D., Gabay,M., Muller, D. A., Triscone, J.-M. and Mannhart, J. Superconducting Interfaces Between Insulating Oxides *Science* **317**, 1196 (2007).

[9] Li, L., Richter, C., Mannhart, J. and Ashoori, R. C. Coexistence of magnetic order and two-dimensional superconductivity at LaAlO3/SrTiO3 interfaces *Nature Phys.* **7**, 762 (2011).

[10] Bert, J. A., Kalisky, B., Bell, C., Kim, M., Hikita, Y., Hwang, H. Y. and Moler, K. A. Direct imaging of the coexistence of ferromagnetism and superconductivity at the LaAlO3/SrTiO3 interface *Nature Phys.* **7**, 767 (2011).

[11] Gibert, M., Zubko, P., Scherwitl, R., Iniguez, J., and Triscone, J. -M. Exchange bias in $LaNiO_3$-$LaMnO_3$ superlattices *Nature Mater.* **11**, 195 (2012).

[12] Kaiser, A. M., Gray, A. X., Conti, G., Son, J., Greer, A., Perona, A., Rattanachata, A., Saw, A. Y., Bostwick, A., Yang, S., Yang, S.-H., Gullikson, E. M., Kortright, J. B., Stemmer, S. and Fadley, C. S. Suppression of Near-Fermi Level Electronic States at the Interface in a LaNiO3/SrTiO3 Superlattice *Phys. Rev. Lett.* **107**, 116402 (2011).

[13] Son, J., LeBeau, J. M., Allen, S. J. and Stemmer, S. Conductivity enhancement of ultrathin LaNiO3 films in superlattices Appl. Phys. Lett. **97**, 202109 (2010).

[14] Boris, A. V., Matiks, Y., Benckiser, E., Frano, A., Popovich, P., Hinkov, V., Wochner, P., Castro-Colin, M., Detemple, E., Malik, V. K., Bernhard, C., Prokscha, T., Suter, A., Salman, Z., Morenzoni, E., Cristiani, G., Habermeier, H.-U. and Keimer, B. Dimensionality Control of Electronic Phase Transitions in Nickel-Oxide Superlattices *Science* **332**, 937 (2011).

[15] May, S. J., Santos, T. S., and Bhattacharya, A. Onset of metallic behavior in strained $(LaNiO_3)_n/(SrMnO_3)_2$ superlattices *Phys. Rev. B* **79**, 115127 (2009).

[16] Hoffman, J., Tung, I. C., Nelson-Cheeseman, B. B., Liu, M., Freeland, J. W., and Bhattacharya, A. Charge transfer and interfacial magnetism in $(LaNiO_3)_n$ $/(LaMnO_3)_2$ superlattices *arXiv:1301.7295* (2013).

[17] Perdew, J. P. and Zunger, A. Self-interaction correction to density-functional approximations for many-electron systems *Phys. Rev. B* **23**, 5048 (1981).

[18] Han, M. J., Marianetti, C. A., and Millis, A. J. Chemical control of orbital polarization in artificially structured transition-metal oxides: La2NiXO6 (X = B , Al, Ga, In) from first principles Phys. Rev. B. **82** 134408, (2010).

[19] http://openmx-square.org.

## Figure Captions

1. The calculated Fermi level DOS for various $(m, n)$ combinations of superlattices. The $z$-axis positions of Ni ions are renormalized so that the first $NiO_2$ layer is located at $z = 0$ and the last is located at $z = 1$. (Inset) Four different types of Ni sites existing in the $(LNO)_m/(STO)_n$ superlattice. Dark gray and light blue circles represent Ni and Ti, respectively. Solid and dotted vertical bars in between transition metals represent SrO and LaO layers, respectively. Nickel of type I1 is located in between the $TiO_2$-SrO and LaO-$TiO_2$ layers, type I2 in between $TiO_2$-SrO and LaO-$NiO_2$, and type I3 in between $NiO_2$-LaO and LaO-$TiO_2$. Nickel of type B is in the bulk-like arrangement located in between $NiO_2$-LaO and LaO-$NiO_2$.

2. (a) Projected Ni-$e_g$ DOS in the $(1, 1)$ superlattice. Red (solid) and blue (dashed) lines represent the $d_{3z^2-r^2}$ and $d_{x^2-y^2}$ states, respectively. (b) Projected Ti-$t2g$ DOS in the $(1, 1)$ superlattice. Blue-dashed and red-solid lines represent the $d_{xy}$ and $d_{yz,zx}$ states, respectively. Vertical dotted lines indicate the position of Fermi energy.

3. (a) Tight-binding calculation results for a linear one-dimensional molecular chain for the weight of the central atom $|\langle i_c|E\rangle|^2$ in the energy eigenfunctions $|E\rangle$. The length of the chain corresponds to the thickness of the LNO layer, *i.e.*, $m$ in $(LNO)_m/(STO)_n$. The central position is given by $i_c = m/2$ and $(m + 1)/2$ for even and odd $m$, respectively. Energy unit is in the hopping parameter $t$. (b) Projected $d_{3z^2-r^2}$ DOS for (3,3) case. As expected, the bonding, non-bonding, and anti-bonding characteristics are most clearly seen in the case of (3,3). Type I2, I3, and B states are represented by blue-dotted, green-dashed, and red-solid lines, respectively. The Fermi level is set to be zero. (c) The projected $d_{3z^2-r^2}$ DOS for bulk-type Ni in the (3,3), (4,1), and (5,2) structures. For comparison, type I2 in (2,2) is also shown (red). The Fermi level is set to be zero. The asterisk marks indicate the peak positions.

4. (a) Schematic illustration of DOS reduction at the Fermi level as a function of layer position relative to the interface. The reduced DOS is transfered to the lower energy part. (b) Projected $d_{3z^2-r^2}$ DOS of two interface layer nickels (blue and green) and the inner layer nickel (red) in the (5,2) superlattice. The arrow indicates the amount of DOS reduction.

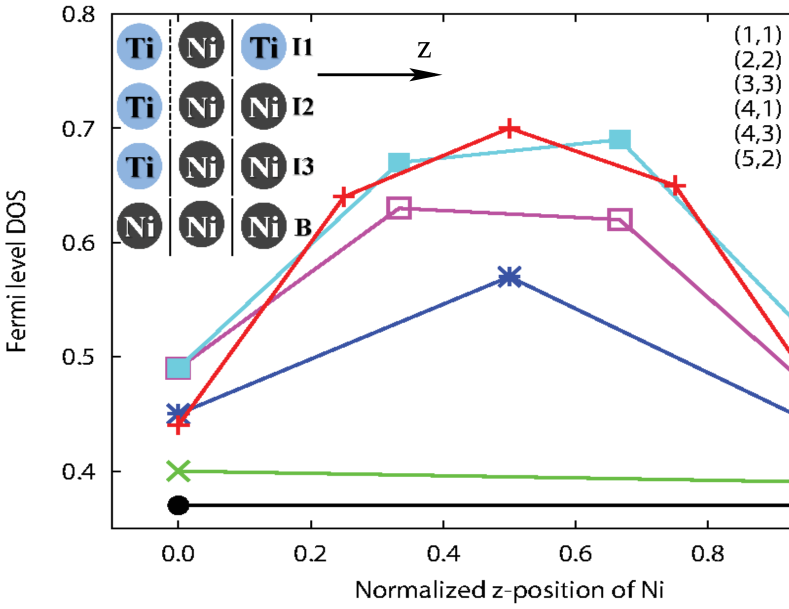

FIG. 1:

Fig.1

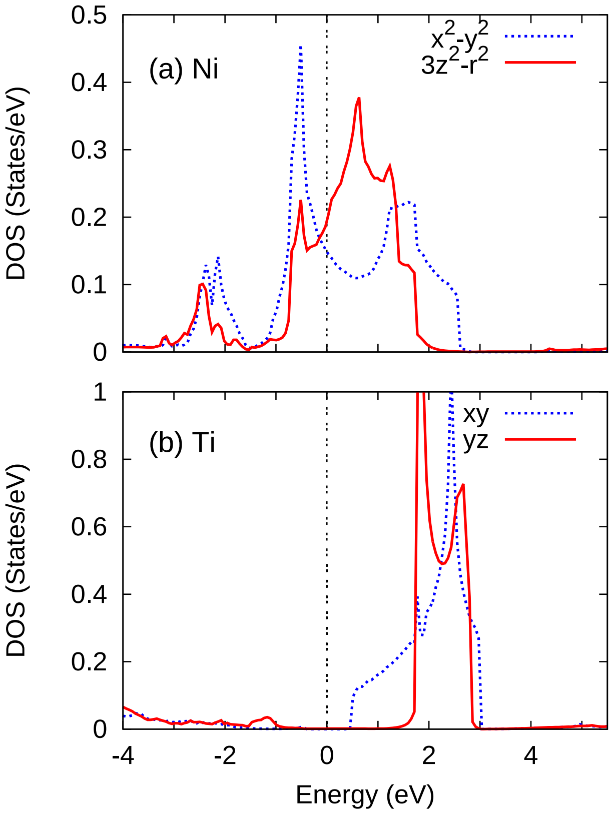

FIG. 2:

Fig.2

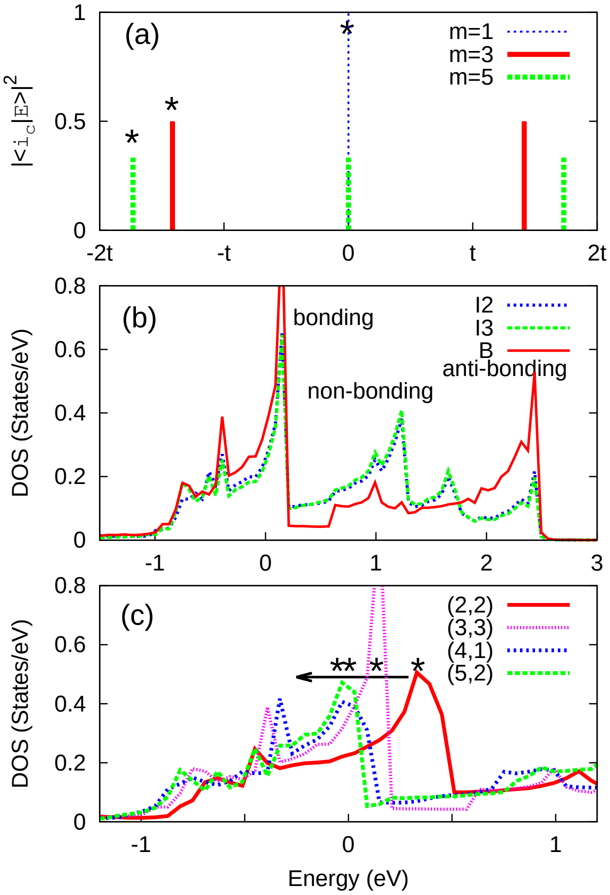

FIG. 3:

Fig.3

Fig.4

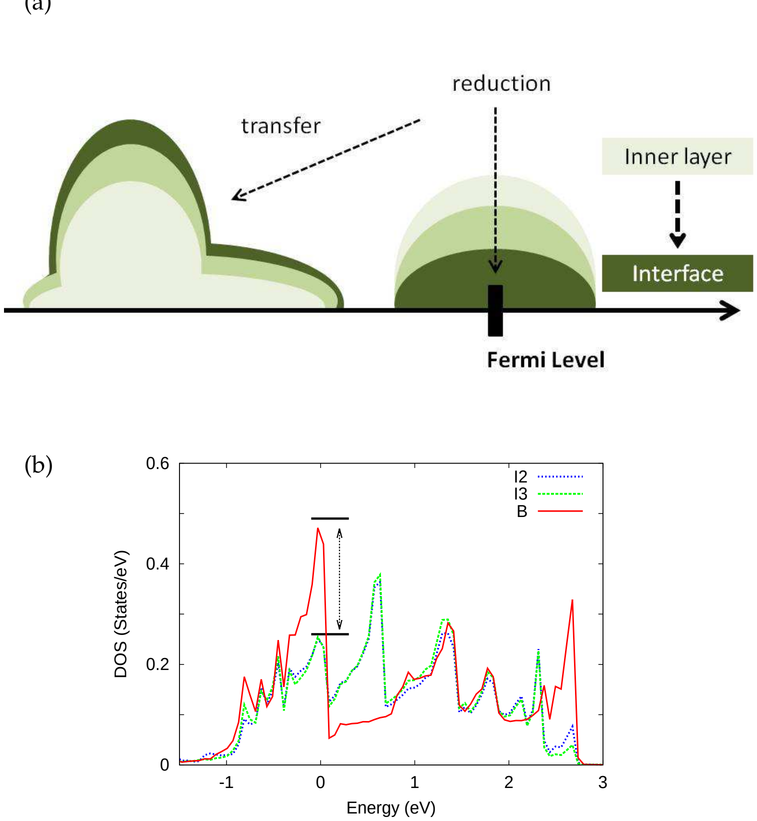
(a)
reduction
transfer
Inner layer
Interface
Fermi Level
(b)
0.6
0.4
0.2
0
DOS (States/eV)
I2
I3
B
-1
0
1
2
3
Energy (eV)

FIG. 4: